AMERICAN SOCIETY FOR MICROBIOLOGY | Journal of Virology

Inhibition of Human Metapneumovirus Binding to Heparan Sulfate Blocks Infection in Human Lung Cells and Airway Tissues

Edita M. Klimyte,[a] Stacy E. Smith,[a] Pasqua Oreste,[b] David Lembo,[c] Rebecca Ellis Dutch[a]

Department of Molecular and Cellular Biochemistry, University of Kentucky, Lexington, Kentucky, USA[a]; Glycores 2000 S.r.l., Milan, Italy[b]; Department of Clinical and Biological Sciences, University of Turin, S. Luigi Gonzaga Hospital, Orbassano, Turin, Italy[c]

ABSTRACT

Human metapneumovirus (HMPV), a recently discovered paramyxovirus, infects nearly 100% of the world population and causes severe respiratory disease in infants, the elderly, and immunocompromised patients. We previously showed that HMPV binds heparan sulfate proteoglycans (HSPGs) and that HMPV binding requires only the viral fusion (F) protein. To characterize the features of this interaction critical for HMPV binding and the role of this interaction in infection in relevant models, we utilized sulfated polysaccharides, heparan sulfate mimetics, and occluding compounds. Iota-carrageenan demonstrated potent anti-HMPV activity by inhibiting binding to lung cells mediated by the F protein. Furthermore, analysis of a minilibrary of variably sulfated derivatives of *Escherichia coli* K5 polysaccharide mimicking the HS structure revealed that the highly O-sulfated K5 polysaccharides inhibited HMPV infection, identifying a potential feature of HS critical for HMPV binding. The peptide dendrimer SB105-A10, which binds HS, reduced binding and infection in an F-dependent manner, suggesting that occlusion of HS at the target cell surface is sufficient to prevent infection. HMPV infection was also inhibited by these compounds during apical infection of polarized airway tissues, suggesting that these interactions take place during HMPV infection in a physiologically relevant model. These results reveal key features of the interaction between HMPV and HS, supporting the hypothesis that apical HS in the airway serves as a binding factor during infection, and HS modulating compounds may serve as a platform for potential antiviral development.

IMPORTANCE

Human metapneumovirus (HMPV) is a paramyxovirus that causes respiratory disease worldwide. It has been previously shown that HMPV requires binding to heparan sulfate on the surfaces of target cells for attachment and infection. In this study, we characterize the key features of this binding interaction using heparan sulfate mimetics, identify an important sulfate modification, and demonstrate that these interactions occur at the apical surface of polarized airway tissues. These findings provide insights into the initial binding step of HMPV infection that has potential for antiviral development.

Acute viral respiratory tract infection is the most frequently observed illness in humans worldwide (1). Human metapneumovirus (HMPV), an enveloped, negative-sense, single-stranded RNA virus in the *Paramyxoviridae* family, is a common cause of both upper and lower respiratory tract infections (2–4). First identified in 2001 in the Netherlands, HMPV is now known to be the cause of respiratory infections in humans since at least 1958 (2). Nearly every person is exposed to HMPV in the first decade of life; seroconversion occurs on average by the age of 5 years, and nearly 100% of individuals test seropositive for antibody reactivity to HMPV antigens by the age of 10 (5). In children, HMPV infection is the second most common cause of hospitalization due to respiratory infection after the closely related respiratory syncytial virus (RSV) (6, 7). Although infants are considered the most vulnerable population to illness from HMPV, adults can develop severe respiratory disease as well, especially the elderly, immunocompromised patients, and individuals with chronic underlying diseases (8–10). In addition to upper respiratory involvement with symptoms typically associated with the common cold, HMPV infection can result in serious lower respiratory syndromes such as pneumonia, bronchitis, and bronchiolitis (3, 11). Due to the recent ability to routinely detect this virus through the inclusion of HMPV in multiplex detection assays, HMPV has been associated with disease outside the respiratory tract in some cases, including viral encephalopathy (12–14) and acute myocarditis (15), from initial respiratory involvement. Despite this tremendous clinical burden, there is no known vaccine to prevent HMPV infection, and treatment options are limited to administering ribavirin, which does not have established efficacy against HMPV infection (16).

Key features of HMPV entry into target cells to establish infection have been characterized recently. HMPV utilizes heparan sulfate (HS) present on the cell surface to bind to target cells (17), followed by clathrin-mediated endocytosis and membrane fusion in endosomes (18). Integrin αVβ1 has also been shown to play a role for efficient HMPV entry (17, 19) and has been proposed to be involved in attachment (20). HS is a negatively charged polysaccharide belonging to the family of glycosaminoglycans composed of repeating disaccharide units formed by glucosamine and glucuronic acid, which can undergo a series of modifications dur-

Received 12 July 2016 **Accepted** 27 July 2016

Accepted manuscript posted online 3 August 2016

Citation Klimyte EM, Smith SE, Oreste P, Lembo D, Dutch RE. 2016. Inhibition of human metapneumovirus binding to heparan sulfate blocks infection in human lung cells and airway tissues. J Virol 90:9237–9250. doi:10.1128/JVI.01362-16.

Editor: T. S. Dermody, University of Pittsburgh School of Medicine

Address correspondence to Rebecca Ellis Dutch, rdutc2@uky.edu.

ing the biosynthesis, leading to very heterogeneous chains. In HS the glucosamine can be N-acetylated, or N-sulfated and O-sulfated, in various positions and to various degrees. Glucuronic acid can also be modified by epimerization.

HSPGs have been implicated in virus-cell interactions for other viruses, including RSV (21–23), human papillomavirus (HPV) (24), herpes simplex virus (HSV) (25–28), human immunodeficiency virus (HIV) (29–31), and others (reviewed in reference 32). We have previously shown that nearly complete reduction in HMPV binding and infection results when HS is removed from the cell surface using heparinases, whereas cells that are able to synthesize only HS, and not any other GAGs, are fully able to bind HMPV (17). Unlike other paramyxoviruses that require two distinct viral glycoproteins to mediate attachment and binding, the fusion protein (F) of HMPV is sufficient for binding and infection (33–35). Recombinant HMPV that does not have the attachment protein (G) or the small hydrophobic protein (SH) is able to bind cells at wild-type (WT) levels via HS (17). Thus, the putative interaction between the HMPV F and HS provides an opportunity for antiviral development.

In this study, we describe the potent anti-HMPV effects of the sulfated polysaccharide, iota-carrageenan, in models of respiratory epithelial cells and polarized airway tissues, indicating that the HS-F interaction is important in physiologically relevant models. To further characterize structural features of HS important for binding by HMPV F, we utilized a minilibrary of variably sulfated derivatives of *Escherichia coli* K5 polysaccharide, which revealed that the critical common feature required for effective inhibition of binding and infection is O-sulfation. In addition, we showed that occluding heparan sulfate with the peptide dendrimer SB105-A10 inhibits the binding interaction between HMPV F and target cells and airway tissues. These results provide additional support for a role for HS-HMPV F protein interactions in physiologically relevant models and identify key features of the interaction between HMPV and HS that have implications for infection *in vivo* and may serve for antiviral development.

MATERIALS AND METHODS

Cells and tissues. Vero cells were grown in Dulbecco modified Eagle medium (Gibco) supplemented with 10% fetal bovine serum (FBS). A549 cells were grown in Roswell Park Memorial Institute medium (RPMI; Lonza) supplemented with 10% FBS. BEAS-2B cells, a human bronchial epithelial cell line, obtained from ATCC, were maintained in BEGM medium containing all the recommended supplements (Lonza) in flasks coated with bovine collagen (Sigma), bovine fibronectin (VWR Scientific) and bovine serum albumin (EMD Millipore). All cells were grown at 37°C under 5% CO_2.

Well-differentiated (transepithelial resistance $>$ 1000 Ω) primary normal bronchial human airway epithelial (HAE) tissue cultures were purchased from MatTek Corp. (Ashland, MA). Cell culture inserts were placed atop two washers (MatTek) in six-well plates with 5 ml of AIR 100 growth medium (MatTek) in contact with the basal surface and incubated at an air-liquid interface at 37°C and 5% CO_2. Tissues were maintained for 5 to 7 days for differentiation after arrival by washing the apical surface with 0.9% sodium chloride and changing the media every 48 h prior to initiation of the infection experiments.

Antibodies. A rabbit polyclonal antibody against avian metapneumovirus (AMPV) C matrix (M) protein supplied by Sagar Goyal (University of Minnesota) with cross-reactivity to HMPV M was used to detect HMPV M protein by Western blotting (36). Antipeptide antibodies to HMPV F (Genemed Synthesis, San Francisco, CA) were generated using amino acids 524 to 538 of HMPV F (37). All other antibodies were purchased from the various companies: β-actin (Sigma) and peroxidase AffiniPure goat anti-rabbit IgG and goat anti-mouse IgG (Jackson ImmunoResearch).

Heparan sulfate mimicking and occluding compounds. Iota-carrageenan was purchased from Sigma (Invitrogen). Peptide dendrimer SB105-A10 ($[H\text{-ASLRVRIKK}]_4$ Lys_2-Lys-β-Ala-OH) was synthesized by Lifetein with a purity of >95%. *Escherichia coli* K5 polysaccharides derivatives were provided by David Lembo and Glycores 2000 (38).

Cell viability assay. Approximately 10,000 BEAS-2B or A549 cells were grown in triplicate overnight in a 96-well plate. BEAS-2B cells were either incubated with 2 μM SB105-A10 for 1 h, 40 μg of iota-carrageenan/ml for 4 h, or 10 μM concentrations of each of the K5 derivatives for 4 h at 37°C. A549 cells were incubated with 2 μM SB105-A10 for 1 h at 37°C. Control cells were incubated with Opti-MEM, which was used to dilute all of the compounds. Then, 3-(4,5-dimethylthiazol-2-yl)-2,5-diphenyl-2*H*-tetrazolium bromide (MTT; Fisher Scientific) (5 mg/ml) was added, followed by incubation for 3 h at 37°C. The medium was removed from the cells by tapping the plate and blotting the excess liquid. Next, 100 μl of stop solution (90% isopropyl alcohol, 10% dimethyl sulfoxide) was added, and the plate was incubated at room temperature for 20 min in the dark with rocking. The absorbance was read at 590 nm using a plate reader. The absorbance of treated cells was normalized to the untreated control.

Virus propagation and titers. The recombinant, green fluorescent protein (GFP)-expressing HMPV (rgHMPV) strain CAN97-83 (genotype group A2) and the mutant viruses HMPV ΔG and HMPV ΔG/ΔSH with a codon-stabilized SH gene (39) were kindly provided by Peter L. Collins and Ursula J. Buchholz (NIAID, Bethesda, MD). The viruses were propagated in Vero cells (starting multiplicity of infection [MOI], 0.01 to 0.03), followed by incubation at 37°C with Opti-MEM, 200 mM L-glutamine, and 0.3 μg of TPCK (tolylsulfonyl phenylalanyl chloromethyl ketone)-trypsin (Sigma)/ml, replenished every day. On day 5, or when cytopathic effects were observed in at least 25% of the cells, the cells and medium were collected and subjected to centrifugation at 2,500 × *g* for 10 min at 4°C on a Sorvall RT7 tabletop centrifuge. The supernatant was then stored in 1× sucrose phosphate glutamate (SPG; 218 mM sucrose, 0.0049 M L-glutamic acid, 0.0038 M KH_2PO_4, 0.0072 M K_2HPO_4), and aliquots were flash frozen in liquid nitrogen and thawed twice prior to storage at −80°C. To achieve more concentrated rgHMPV for HAE tissue experiments, supernatants of harvested cells and medium were subjected to centrifugation on a 20% sucrose cushion for 3 h at 27,000 × *g* at 4°C using a SW28 swinging-bucket rotor on a Beckman Optima L90-K ultracentrifuge. After centrifugation, the supernatant was removed, and the pellet was resuspended in 100 μl of Opti-MEM per T75 flask, harvested, and left at 4°C overnight. Aliquots were stored at −80°C by flash freezing in liquid nitrogen.

Recombinant GFP-expressing parainfluenza virus 5 (rgPIV5) was kindly provided by Robert Lamb (Howard Hughes Medical Institute, Northwestern University) (35). rgPIV5 was propagated in MDBK cells as described previously (40) and stored in 1× SPG. Aliquots were frozen in liquid nitrogen and thawed twice prior to storage at −80°C.

For GFP-expressing viruses (rgHMPV and rgPIV5), viral titers were calculated by creating serial dilutions of the viral samples in Opti-MEM. Vero cells were seeded on a 96-well plate overnight and infected in serial dilution (10^{-1} to 10^{-12}) with 50 μl of virus solution in duplicate. The number of GFP-expressing cells was counted in wells demonstrating 25 to 100 GFP-positive cells the following day. The average titer was calculated based on the dilution of the virus solution in the wells counted.

For non-GFP expressing viruses (HMPV ΔG and HMPV ΔG/ΔSH) viral particles were estimated using serial dilutions of viral samples assessed for M protein content using Western blotting and compared to protein levels of an rgHMPV standard of known titer. The volumes of untitered virus and the rgHMPV standard of a known concentration (2, 4, and 8 μl in duplicate) were resolved using SDS–15% PAGE, and the proteins were transferred to a polyvinylidene difluoride membrane (Fisher)

at 50 V for 80 min. The membrane was blocked with Odyssey blocking buffer (Li-Cor) at 4°C overnight, followed by incubation with anti-AMPV M antibody (1:500) in PCT (phosphate-buffered saline [PBS; Invitrogen] with casein and 0.2% Tween 20) for 3 h at room temperature. The membrane was washed with t-TBS (0.2% Tween 20 in 1× TBS [Tris-buffered saline]) and incubated with peroxidase AffiniPure goat anti-rabbit secondary antibody (1:10,000) in PCT for 1 h at room temperature. The membrane was washed with t-TBS and incubated with SuperSignal West Pico chemiluminescent substrate (Fisher) for 10 min in the dark prior to development by using enhanced chemiluminescence. Densitometry was quantified using ImageQuant TL, and an average density units of M protein per μl of virus input was calculated for each sample. The titer was determined by comparing to the standard of known titer.

Cell infection assay. BEAS-2B cells were grown to low confluence (approximately 50,000 cells per well [as recommended by the American Type Culture Collection]) in a 24-well plate overnight. Iota-carrageenan solution was freshly prepared in PBS at 0.7 mg/ml by incubation at 55°C with brief vortexing. The virus was pretreated with iota-carrageenan or K5 polysaccharide derivatives diluted in Opti-MEM for 30 min at 4°C with rocking. The cells were washed two times with PBS, and 200 μl of virus solution was added at an MOI of 1. For SB105-A10 experiments, BEAS-2B or A549 cells were washed twice with PBS, followed by incubation with 200 μl of SB105-A10 diluted in Opti-MEM at variable concentrations at 37°C for 1 h. The cells were washed once with PBS and infected with 200 μl of virus solution in Opti-MEM at an MOI of 1. For all treatments, the cells were incubated with the infection media in duplicate for 2 h at 37°C with rocking every 30 min. After 2 h, the cells were washed twice with PBS, and the infection medium was replaced. For GFP-expressing virus, after an overnight incubation, the cells were resuspended, fixed in 2% formaldehyde diluted in PBS with 50 mM EDTA, and analyzed with a BD FACSCalibur flow cytometer, for which the GFP expression of at least 10,000 cells was determined. Data analysis was performed using FCS Express software, and the data presented in the graphs represent the percentage of GFP-expressing cells as a percentage of the untreated control as previously described (17).

HAE infection assay. HAE tissues were maintained according to the manufacturer's recommendations for 5 to 7 days after arrival. The tissues were transferred to a new six-well plate with 1 ml of HEPES-buffered saline (HBS; 150 mM NaCl, 20 mM HEPES [pH 7.5], 1 mM $MgCl_2$, 1 mM $CaCl_2$) and washed with 400 μl of sterile 0.9% NaCl. The apical surface was washed three times with 75 μg of lysophosphatidylcholine (LPC; Sigma)/ml in HBS for 10 min at room temperature (41). LPC was removed from the apical surface, and HBS was removed from the basal surfaces of the tissues, and 1 ml of AIR 100 growth medium was added to the basal side. To measure the effects of heparan sulfate mimics, rgHMPV or rgPIV5 at an MOI of 5 (this calculation was based on 0.8×10^6 cells per tissue according to the manufacturer) was pretreated either with 40 μg of iota-carrageenan/ml, 10 μM K5-N,OS (H), or 10 μM K5-OS(H) (untreated control received Opti-MEM) in a total volume of 100 μl. For SB105-A10, the tissues were treated with 2 μM SB105-A10 in Opti-MEM for 1 h at 37°C prior to infection (untreated control tissue was incubated with Opti-MEM). The infection solution (100 μl at an MOI of 5) was added to the apical surface of the tissues dropwise, and the tissues were incubated at 37°C for 2 h with rocking every 30 min. After 2 h, the infection medium was aspirated, and the apical surface washed 1× with 200 μl of HBS. Fresh AIR 100 growth medium with 0.3 μg of TPCK-trypsin/ml was added to each well, followed by incubation at 37°C. After 48 h, the apical surfaces of the tissues were imaged for GFP expression using an Axiovert-100 (three fields per tissue) at ×5 magnification. The number of infected cells was determined by counting the GFP-expressing cells and then averaged per tissue. The results are reported as the percent infection of the untreated control.

Cell binding assay. Approximately 250,000 BEAS-2B cells were cultured overnight in a six-well plate. rgHMPV was pretreated with iota-carrageenan at 40 μg/ml or a 1 μM concentration of the K5 polysaccharide derivatives diluted in Opti-MEM for 30 min at 4°C with rocking. For SB105-A10 treatment, the cells were washed twice with PBS, followed by incubation in a 200-μl solution of SB105-A10 diluted in Opti-MEM at 37°C for 1 h. For all treatments, the cells were washed twice with cold PBS and infected with 500 μl of virus solution at an MOI of 1 for 2 h at 4°C with rocking to prevent internalization. The cells were washed with PBS three times, lysed using 45 μl of RIPA buffer with 0.15 M NaCl with a complete protease inhibitor cocktail tablet (Fisher), and frozen at −20°C. The cells were thawed and scraped on ice, and the lysates were cleared by centrifugation for 10 min at 55,000 rpm at 4°C (Sorvall Discovery M120). Western blot analysis for M to quantify bound HMPV was carried out as described above.

Statistical analysis. All data are presented as means ± the standard deviations of a minimum of three independent experiments. A standard Student *t* test or one-way analysis of variance (ANOVA) was performed when appropriate to analyze the differences between the individual experiments with statistical significance set as $P \leq 0.05$. A post hoc Bonferroni's multiple-comparison test (GraphPad Prism) was used within one-way ANOVA to identify specific differences between groups.

RESULTS

Iota-carrageenan inhibits HMPV infection in human respiratory cells. To dissect how interaction with HS regulates HMPV infection in physiologically relevant models and to determine whether blocking this interaction could be a potential antiviral approach, we utilized a sulfated polysaccharide, heparan sulfate mimetics and a compound that occludes HS in combination with infection studies in human bronchial epithelial cells (BEAS-2B) or human airway epithelial (HAE) models. Sulfated polysaccharides have been previously used to target viral infection, including a number of studies with carrageenans, which are isolated from red seaweed (42). Carrageenans are composed of sulfated repeating galactose units (Fig. 1B). The three types of known carrageenans (iota, lambda, and kappa) differ in number and positions of sulfate groups (reviewed in reference 42). Carrageenans have shown antiviral activity against a number of viral pathogens, including HPV (43), HIV (44), dengue virus (45), and influenza A virus (46). Importantly, iota-carrageenan has been used safely in human trials in the form of a nasal spray to reduce viral infection (47–49).

To verify that sulfated polysaccharides would inhibit HMPV infection in a relevant cell culture model, we first determined the anti-HMPV activity of iota-carrageenan, a well-characterized sulfated polysaccharide that has been shown to inhibit the infection of other viruses that bind HS. Infection of BEAS-2B cells was performed using a recombinant HMPV (strain CAN97-83, clade A2) that results in green fluorescent protein (GFP) expression as a surrogate measure for infectivity, which was quantified by flow cytometry. Pretreatment of HMPV with iota-carrageenan resulted in inhibition of infection, with nearly a complete reduction in infection achieved with 10 μg of iota-carrageenan/ml (Fig. 2A and C). To determine whether iota-carrageenan had a nonspecific antiviral effect, paramyxovirus parainfluenza virus 5 (PIV5), which does not utilize HS for binding, was used. Incubating rgPIV5, a recombinant PIV5 virus that results in GFP expression, with iota-carrageenan prior to infection did not inhibit infection of BEAS-2B cells at any of the concentrations used compared to the untreated control (Fig. 2B and C). Similar effects of iota-carrageenan on rgHMPV and rgPIV5 infection were observed in Vero cells (data not shown). These results indicate that HS-HMPV interactions are critical in BEAS-2B cells and that iota-

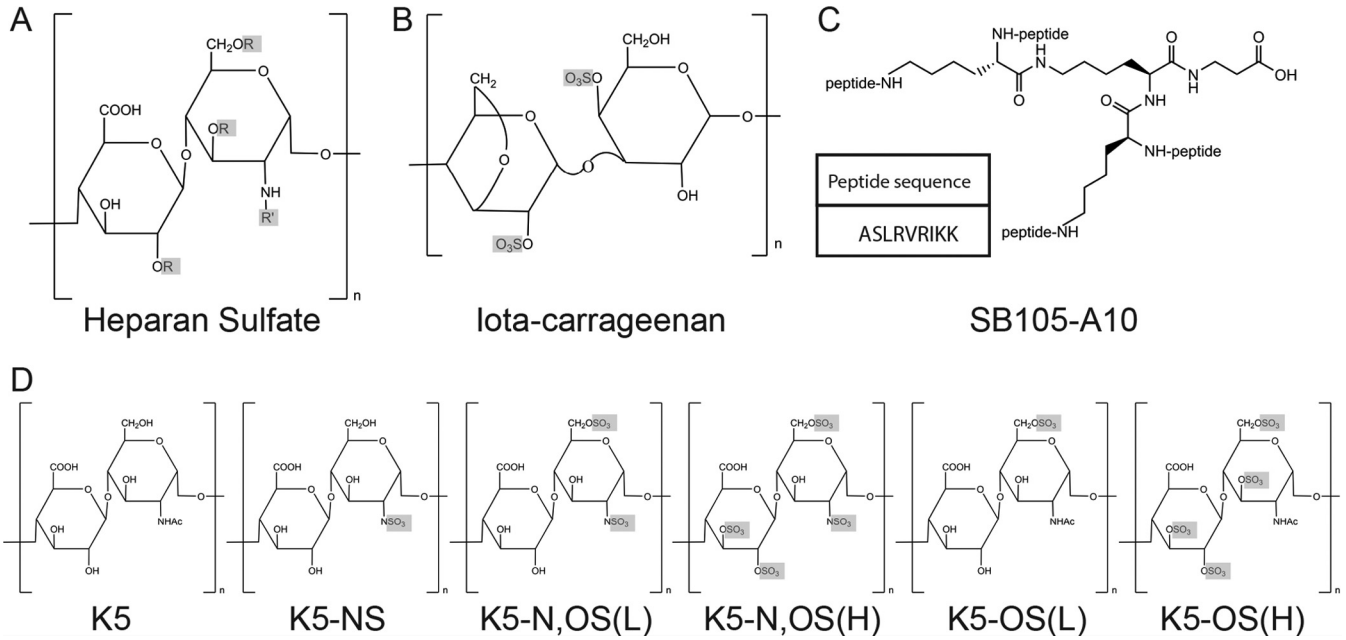

FIG 1 Representative structures. (A) Heparan sulfate disaccharides modified by the following possible substitutions: Ac = acetyl; R = H or $SO3^{-}$; R′ = H, Ac, or SO_3^{-} (60). (B) Iota-carrageenan structure (42). (C) SB105-A10. (D) K5 polysaccharide derivatives.

carrageenan has anti-HMPV activity, most likely attributed to its sulfated structure.

Our previous studies suggested that HMPV binds to HS via the F protein, and we hypothesized that iota-carrageenan is inhibiting HMPV infection by competing with HS binding sites located in HMPV F. To test this, HMPV was added to BEAS-2B cells at 4°C, allowing for binding to occur but not infection, and the amount of bound virus was quantified by detection of the HMPV matrix protein present in cell lysates by Western blotting, with β-actin as a loading control. Pretreating HMPV at an MOI of 1 with 40 μg of carrageenan/ml for 30 min at 4°C prior to addition to the cells resulted in about 85% inhibition of particle binding compared to the untreated control (Fig. 2D and E), demonstrating that iota-carrageenan competes with the binding of HMPV to HS. Of the three glycoproteins in the viral envelope of HMPV (the attachment protein G, the small hydrophobic protein SH, and F), only F is required by HMPV to be infectious; recombinant HMPVs without G or SH, HMPV ΔG and ΔGΔSH, respectively, are able to bind cells at wild-type levels (17) and are replication competent in a nonhuman primate model of infection (34). To test whether iota-carrageenan inhibition of HMPV binding and infection is dependent exclusively on F, we pretreated the recombinant HMPV ΔG and ΔGΔSH with iota-carrageenan and determined the effects on overall infection and binding in BEAS-2B cells. Iota-carrageen inhibited HMPV ΔG and ΔGΔSH binding to a degree similar to that demonstrated by wild-type HMPV (Fig. 2D and E), which supports the hypothesis that interaction between HMPV and HS is mediated by F. Interestingly, a greater fraction of input particles of ΔG and ΔGΔSH HMPV than WT HMPV bound to BEAS-2B cells, suggesting that ΔG and ΔGΔSH HMPV binding to BEAS-2B cells was more efficient on a per particle basis (Fig. 3A). The input number of particles for all three virus samples was verified for each experiment and was not statistically different across all binding assays completed (Fig. 3B), demonstrating that increases in particle numbers did not cause the observed increase in binding for ΔG and ΔGΔSH HMPV. To address the possibility that the ΔG and ΔGΔSH recombinant viruses had greater F content that contributes to increased binding in BEAS-2B cells, the ratio of F to M protein in WT, ΔG, and ΔGΔSH HMPVs was determined by Western blotting (Fig. 3C). No difference in the F/M ratio was detected between WT HMPV and the recombinant viruses, indicating that increased binding is not due to increased per particle F protein levels (Fig. 3D). Thus, the reasons for these unexpected results remain to be determined. However, despite increased binding at the baseline, iota-carrageenan did inhibit the binding of ΔG and ΔGΔSH HMPVs to the same degree as did WT HMPV (Fig. 2E). These findings suggest that iota-carrageenan inhibits the binding of WT and recombinant HMPVs without G and SH in a manner that is dependent on F and not the other surface glycoproteins.

The results in a monolayer respiratory cell model support the hypothesis that HMPV F mediates a key binding interaction to HS, and this event can be inhibited using the highly sulfated polysaccharide, iota-carrageenan. However, a monolayer cell culture model is limited in the ability to recapitulate the complex features of the respiratory epithelium, which include moving cilia, mucus, distinct cell types with important physiological roles, and polarity maintained by tight junctions. Furthermore, immortalized cells highly express HSPGs in a pattern that may be different than complex organized tissues found *in vivo*, and immunohistochemistry studies have not detected significant amounts of HS on the apical surface of human airway, raising concerns that HS interactions may be less important in an airway model (50). We therefore examined the effect of sulfated polysaccharides in a polarized human airway tissue model (HAE; MatTek) that more closely recapitulates the complexity of the human airway, which is the primary site of HMPV infection. HAE tissues have been previously used as models of respiratory virus infection, including human

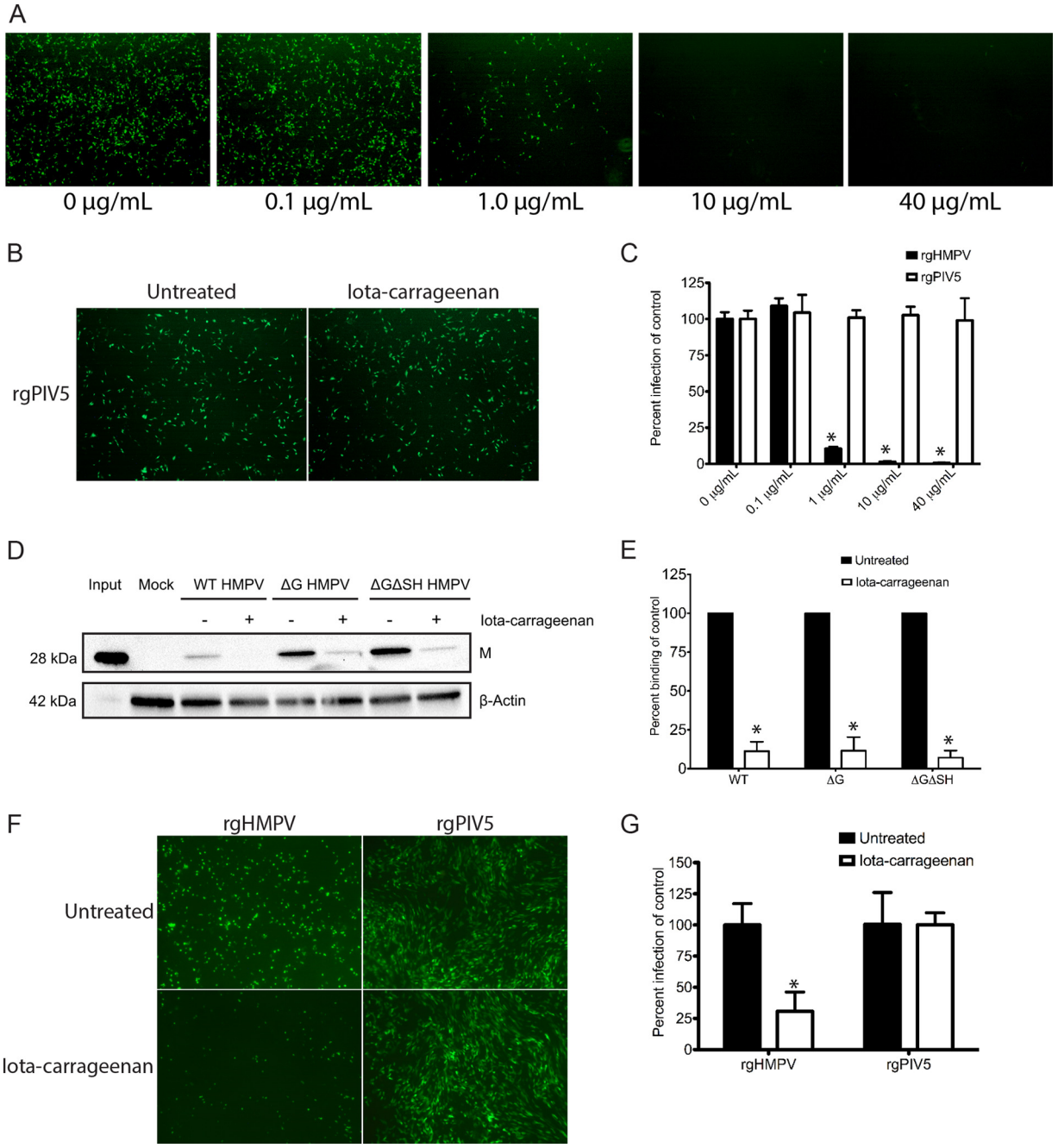

FIG 2 Iota-carrageenan inhibits HMPV infection in cells and tissues by blocking binding. (A) BEAS-2B cells infected with rgHMPV at an MOI of 1 was treated with variable concentrations of iota-carrageenan. Cells were imaged 24 HPI. (B) BEAS-2B cells were infected with rgPIV5 at an MOI of 1 treated with 40 μg of iota-carrageenan/ml or vehicle. Cells were imaged at 24 h postinfection. (C) Quantification of rgHMPV and rgPIV5 infection in BEAS-2B cells using flow cytometry to detect GFP expressing cells 24 h postinfection. The data are presented as a percent infection of the untreated control (0 μg/ml) for each virus. Data points are means ± the standard deviations of duplicate measurements and are representative of a minimum of three independent experiments. *, Statistical significance ($P < 0.0001$). (D) HMPV viruses (WT and recombinant mutants ΔG and ΔGΔSH) were treated with vehicle or 40 μg of iota-carrageenan/ml and added to BEAS-2B cells at an MOI of 1 at 4°C for particle binding. Lysates of washed cells were analyzed for HMPV binding by Western blotting for M. Input represents 5% WT HMPV was added to the cells for binding. No virus was added to mock-infected cells. β-Actin served as a loading control. (E) Band intensities of the matrix protein and β-actin were determined for untreated and treated (40 μg/ml iota-carrageenan) samples. The data are reported as a ratio of M to β-actin normalized to the untreated control for each virus. Data points are means ± the standard deviations of measurements representative of seven independent experiments. *, Statistical significance ($P < 0.0001$). (F) HAE tissues were infected with rgHMPV or rgPIV5 at an MOI of 5 treated with 40 μg of iota-carrageenan/ml or vehicle and imaged at 48 h postinfection at ×5 magnification. (G) Quantification of HAE tissue infection. Data points are means ± the standard deviations of triplicate measurements and are representative of a minimum three independent HMPV infection experiments. *, Statistical significance ($P < 0.0001$).

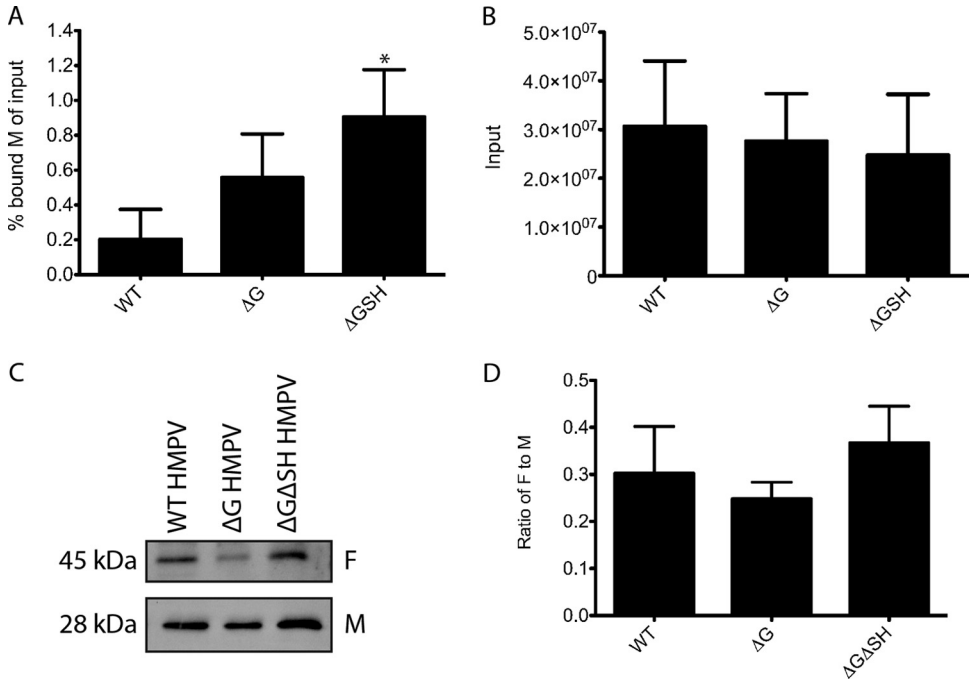

FIG 3 Recombinant ΔG and ΔGΔSH HMPV exhibit enhanced binding to BEAS-2B cells compared to WT HMPV. (A) HMPV viruses (WT and recombinant mutants ΔG and ΔGΔSH) were added to BEAS-2B cells at an MOI of 1 at 4°C for particle binding. Lysates of washed cells and 5% of each virus volume added to cells for binding were analyzed for HMPV binding by Western blotting for M. The band intensities of the matrix protein and β-actin were determined for input and bound. The data are reported as a ratio of the percent bound M to the input. Data points are means ± the standard deviations of measurements representative of five independent experiments. *, Statistical significance ($P < 0.05$). (B) The input of the three viruses was determined by Western blotting by detection of M and quantified by calculating the band intensity. The data are reported as an estimated number of particles added to cells in the binding assays. Data points are means ± the standard deviations of measurements representative of three different experiments. (C) HMPV viruses (WT and recombinant mutants ΔG and ΔGΔSH) were analyzed by Western blotting for F and M. (D) The relative band intensities were quantified. The data are reported as a ratio of the mean F to the mean M abundance and are representative of three independent experiments.

parainfluenza virus 3 (51), rhinovirus (52), human bocavirus 1 (53), and RSV (54).

To test whether iota-carrageenan inhibits HMPV infection in the HAE model, iota-carrageenan-treated rgHMPV was used to inoculate the apical surfaces of the HAE tissues, and a significant reduction in infection of approximately 75% was observed (Fig. 2F and G). Unlike rgHMPV, treatment of rgPIV5 with iota-carrageenan had no effect on infection in the airway tissues (Fig. 2F and G). These findings indicate that HMPV interactions with HS are also important in complex polarized airway tissues that histologically resemble the human respiratory tract and support the hypothesis that HMPV requires HS to establish infection at the apical surface of the respiratory epithelium.

O-sulfated K5 polysaccharide derivatives inhibit HMPV infection. Although our preliminary results strongly support a key role for HS in HMPV infection, the specific features of HS required remain to be determined. A class of molecules mimicking HS and thus possible inhibitors of HS-virus interactions is represented by the sulfated derivatives of the *E. coli* capsular K5 polysaccharide (Fig. 1D). K5 polysaccharide derivatives are heparan-like molecules devoid of anticoagulant activity obtained by the sulfation of the *E. coli* capsular K5 polysaccharide that has the same structure of the biosynthetic precursor of HS, *N*-acetyl heparosan. A small library of derivatives with different degrees of sulfation has been synthesized using chemical and enzymatic modifications (38). Sulfated K5 derivatives have been shown to inhibit infection in other viruses in a specific manner, including HPV (43), RSV (55), dengue virus (56), cytomegalovirus (CMV) (57), HSV-1 and HSV-2 (58), and HIV (59). Analysis of the anti-HMPV activity of these compounds can therefore be used to identify structural features that are important for recognition by HMPV F and potentially help to identify a potent HS mimic.

Because HS is negatively charged due to sulfate modifications on the disaccharide units, we hypothesized that charge-charge interactions contribute to the binding between F and this polysaccharide. Therefore, we predicted that the most highly sulfated K5 derivatives, mainly K5-N,OS(H), and K5-OS(H), would have the greatest inhibitory effect on HMPV infection. To test this, rgHMPV at an MOI of 1 pretreated with the derivatives at 1 μM was used to inoculate BEAS-2B cells. As predicted, the highly sulfated K5 derivatives, K5-N,OS(H) and K5-OS(H), dramatically inhibited infection (Fig. 4A). Among the lower sulfated derivatives, K5 and K5-NS did not have an observable effect on HMPV infection when examined by microscopy (Fig. 4A), whereas K5-N,OS(L) and K5-OS(L) (Fig. 1D) also inhibited HMPV infection dramatically. K5-NS, which has a single sulfate in position 2 of glucosamine, had no effect on HMPV infection (Fig. 4A), indicating a key role of O-sulfate groups in the observed inhibition. When HMPV was treated with variable concentrations (10 nm to 1 μM) of the K5 derivatives and used to infect BEAS-2B cells, flow cytometry analysis of infected cells revealed a dose-dependent inhibition of HMPV infection by all the O-sulfated K5 derivatives (Fig. 4B). K5-NS had no effect on HMPV infection, whereas some inhibition resulted from K5, although only at the highest concen-

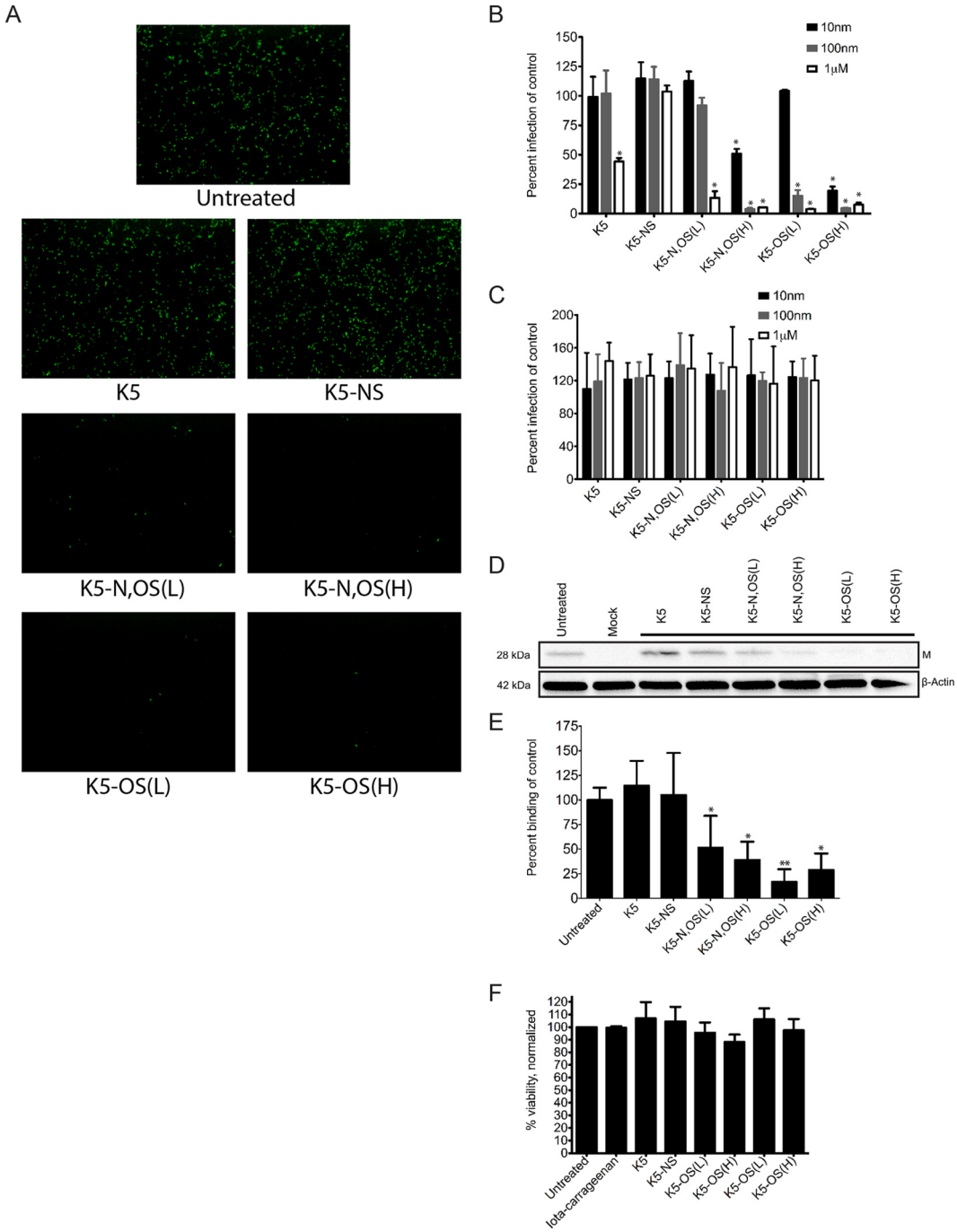

FIG 4 O-sulfated K5 polysaccharide derivatives inhibit HMPV infection in BEAS-2B cells by competing for binding. (A) BEAS-2B cells were infected with rgHMPV at an MOI of 1 treated with a 1 μM concentration of each K5 polysaccharide derivative or vehicle. The cells were imaged at 24 h postinfection. BEAS-2B cells were infected with rgHMPV (B) or rgPIV5 (C) at an MOI of 1 treated with a 10 nM, 100 nM, or 1 μM concentration of each K5 polysaccharide derivative or vehicle. Infection was quantified by flow cytometry to detect GFP-expressing cells at 24 h postinfection. The data are presented as the percent infection of the untreated control. Data points are means ± the standard deviations of duplicate measurements and are representative of a minimum of three independent experiments. Single (*) and double (**) asterisks indicate statistical significances of $P < 0.01$ and $P < 0.0001$, respectively. (D) WT HMPV was treated with vehicle (untreated) or a K5 polysaccharide derivative at 1 μM and added to BEAS-2B cells at an MOI of 1 at 4°C for particle binding. Lysates of washed cells were analyzed for HMPV binding by Western blotting for M. No virus was added to mock-infected cells. β-Actin served as a loading control. (E) Band intensities of the matrix protein and β-actin were determined for untreated and treated (1 μM) samples. The data are reported as a ratio of M to β-actin normalized to the untreated control for each virus. Data points are means ± the standard deviations of measurements representative of five independent experiments. *, Statistical significance of $P < 0.001$; **, statistical significance of $P < 0.0001$. (F) BEAS-2B cells were treated with 40 μg of iota-carrageenan/ml, 10 μM concentrations of each of the K5 polysaccharide derivatives, or vehicle (untreated) in triplicate and assayed for viability by using an MTT cell viability assay according to the manufacturer's protocol. The absorbance at 590 nm was normalized to the untreated control. Data points are means ± the standard deviations of triplicate measurements and are representative of three independent experiments.

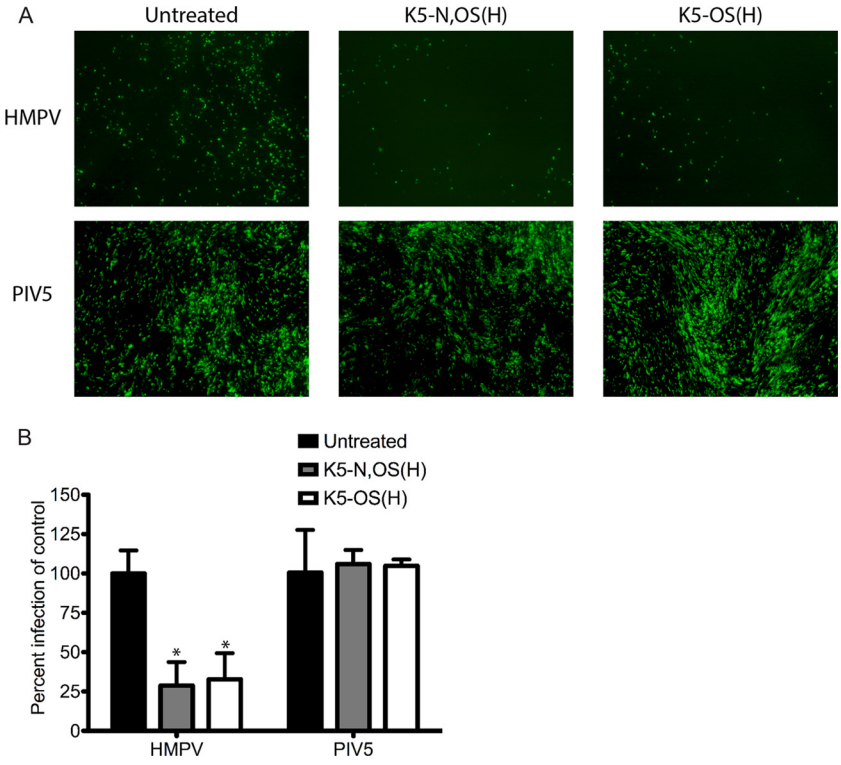

FIG 5 Highly sulfated K5 polysaccharide derivatives inhibit HMPV infection in HAE. (A) HAE tissues were infected with rgHMPV or rgPIV5 at an MOI of 5 treated with 10 μM K5-N,OS(H) or K5-OS(H) or with vehicle (untreated) and imaged at 48 h postinfection at ×5 magnification. (B) Quantification of HAE tissue infection. Data points are means ± the standard deviations of triplicate measurements and are representative of a minimum of three independent experiments. *, Statistical significance ($P < 0.0001$).

tration (Fig. 4B). The reduction of infection by the K5 polysaccharide was not expected, and the mechanism of this action remains unclear since it did not affect HMPV binding (Fig. 4D and E). None of the K5 polysaccharide derivatives had an effect on PIV5 infection (Fig. 4C). In addition, treatment of BEAS-2B cells with a 10 μM concentration of the K5 polysaccharide derivatives, the concentration used in HAE infection experiments and 10-fold higher than the highest concentration used in cell infection assays, did not reduce cell viability, as measured by an MTT cell viability assay (Fig. 4F). Similarly, treatment of BEAS-2B cells with the highest concentration of iota-carrageenan tested in the infection assays did not reduce cell viability, demonstrating that its antiviral activity is not a consequence of cytotoxicity (Fig. 4F). To determine whether the K5 compounds inhibit HMPV infection by competition, the binding assay described in the carrageenan studies was used. rgHMPV was treated with a 1 μM concentration of each of the K5 polysaccharide derivatives prior to incubation with BEAS-2B cells at 4°C at an MOI of 1 to allow for binding to take place. Although unmodified K5 and K5-NS, which have a single N-linked sulfation modification, had no effect on viral binding, the higher-sulfated compounds, K5-N,OS(L) and K5-OS(L), and the highly sulfated compounds K5-N,OS(H) and K5-OS(H) reduced HMPV binding to BEAS-2B cells significantly (Fig. 4E).

To confirm these findings in a physiologically relevant tissue model, we determined the effect of K5-N,OS(H) and K5-OS(H), which had the greatest inhibition of HMPV infection in monolayer cells, in polarized airway tissues. HAE tissues were infected at the apical surface with rgHMPV or rgPIV5 at an MOI of 5 pretreated with 10 μM K5-N,OS(H) or K5-OS(H), or Opti-MEM. At 48 h postinfection, we observed a dramatic reduction in infected cells at the apical surface (Fig. 5A). Quantification of GFP-expressing cells revealed an approximately 70% reduction in HMPV infection compared to the control (Fig. 5B), whereas PIV5 infection was not reduced (Fig. 5A and B). Taken together, these data suggest that highly sulfated K5 derivatives effectively inhibit binding and infection of HMPV and that O-sulfation is an important structural feature required for the interaction to occur, and thus these findings strongly support the hypothesis that HMPV interaction with HS plays a significant role during apical infection. However, for *in vivo* utility, it is likely such compounds would require optimization to achieve a higher degree of inhibition of infection.

Heparan sulfate occlusion inhibits HMPV infection and binding. We have shown that HMPV F mediates a binding interaction to HS that can be inhibited both in cell culture and tissue models using iota-carrageenan and a small library of K5 polysaccharide derivatives. As an alternative mechanism to characterize the interaction between HMPV and HS, we examined the effect of blocking HS moieties on the target cell, thus making heparan sulfate unavailable for binding. There is a 2-fold logic to investigating the effect of a heparan sulfate-occluding compound on HMPV binding. The removal of HS caused a robust block in HMPV infection (17); however, HSPGs have critical constitutive and induced interactions with other cellular proteins (reviewed in reference 60), and removing HS may interrupt these interactions, causing cellular changes. HS occluding compounds that prevent

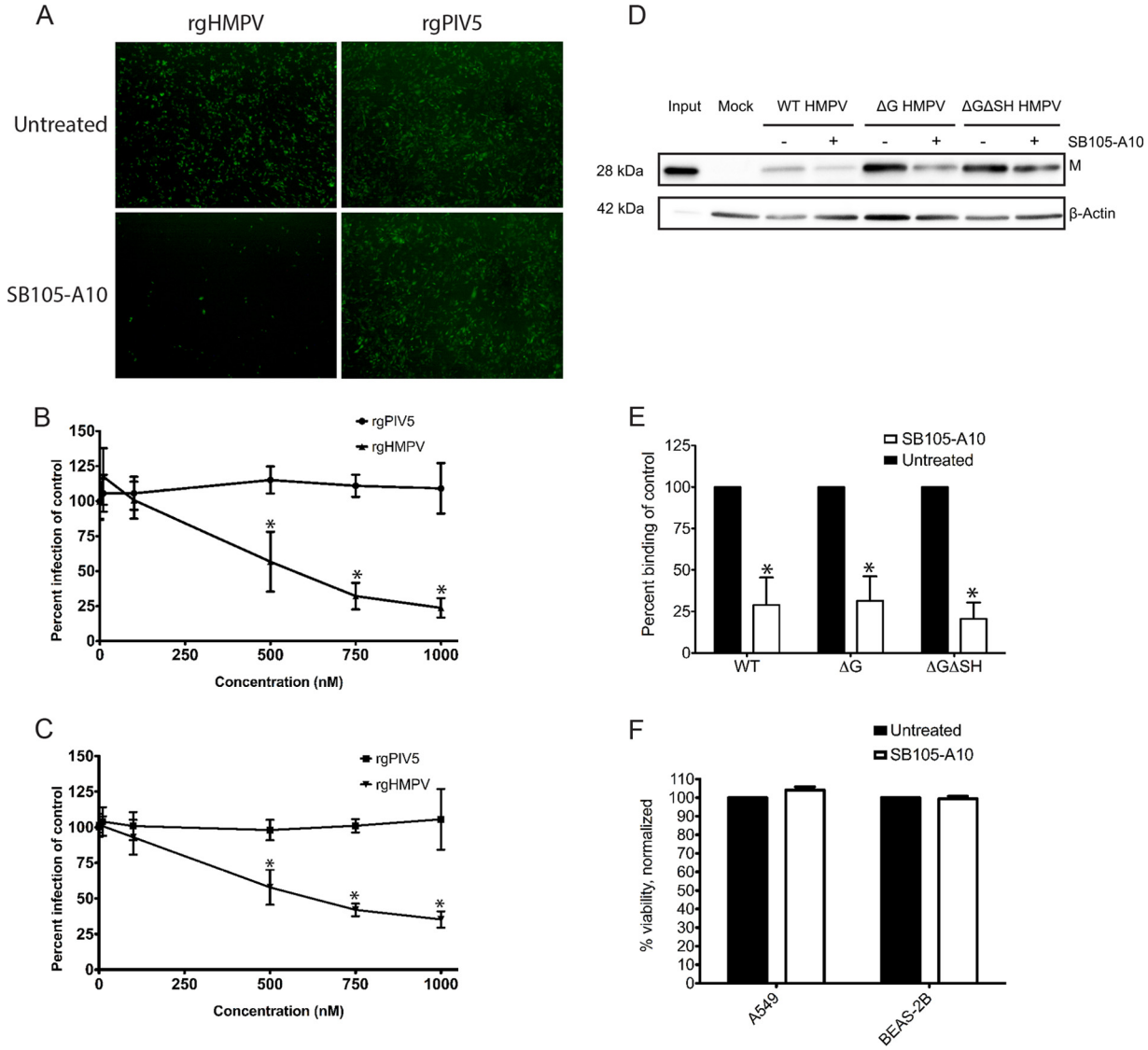

FIG 6 Peptide dendrimer SB105-A10 inhibits HMPV infection in human lung cells by inhibiting binding. (A) BEAS-2B cells treated with 1 μM SB105-A10 or vehicle were infected with rgHMPV or rgPIV5 at an MOI of 1. The cells were imaged at 24 h postinfection. The percent infection of rgHMPV and rgPIV5 at an MOI of 1 treated with variable concentrations of SB105-A10 in BEAS-2B (B) and A549 (C) cells was quantified using flow cytometry. The percent infection is reported normalized to the untreated control for each virus type. Data points are means ± the standard deviations of duplicate measurements and are representative of a minimum of three independent experiments. An asterisk (*) indicates statistical significance ($P < 0.0001$). (D) HMPV viruses (WT and recombinant mutants ΔG and ΔGΔSH) were added to BEAS-2B cells treated with vehicle or with 1 μM SB105-A10 at an MOI of 1 at 4°C for particle binding. Lysates of washed cells were analyzed for HMPV binding by Western blotting for M. Input represents 5% of WT HMPV added to the cells for binding. No virus was added to mock-infected cells. β-Actin served as a loading control. (E) Band intensities of the matrix protein and β-actin were determined for untreated and treated (1 μM SB105-A10) samples. The data are reported as a ratio of M to β-actin normalized to the untreated control for each virus. Data points are means ± the standard deviations of measurements representative of five independent experiments. *, Statistical significance ($P < 0.0002$). (F) BEAS-2B and A549 cells were treated with 2 μM SB105-A10 or vehicle (untreated) and assayed for viability by using an MTT assay. The absorbance at 590 nm was normalized to the untreated control. Data points are means ± the standard deviations of triplicate measurements and are representative of three independent experiments.

further ligand binding are less likely to disrupt preexisting HS interactions and therefore serve as an alternative approach to address the direct interaction of HMPV with HS. Furthermore, a compound that occludes HS and inhibits HMPV infection may serve as a potential building block for antiviral development for HMPV and other viruses that are known to bind HS.

To accomplish this, we utilized a previously characterized heparan sulfate occluding compound, peptide dendrimer SB105-A10 (54, 61, 62). Peptide dendrimers, branched synthetic molecules that consist of a peptidyl branching core and covalently attached surface peptide units, have a number of potential applications, especially in relation to the development of antiviral agents. The peptide dendrimer SB105-A10 (Fig. 1C), which has a branched peptide core with clusters of basic residues that bind to negatively charged sulfate and carboxyl groups, has been shown to specifically occlude ligand binding from HSPGs (61, 62). Further-

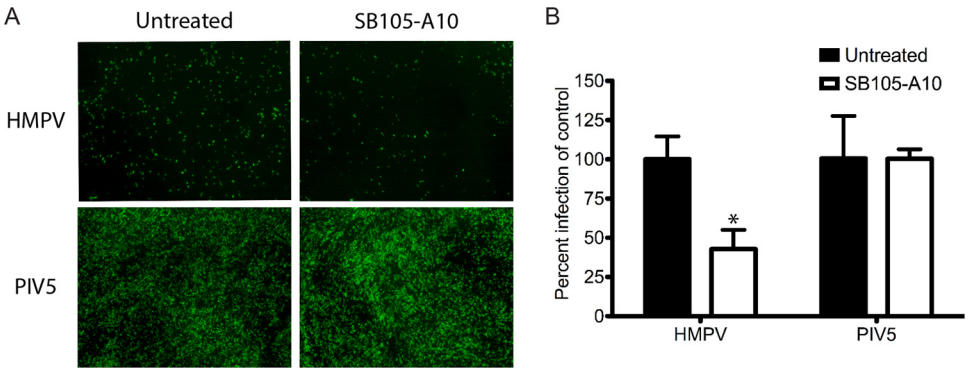

FIG 7 Treatment of HAE tissues with SB105-A10 reduces HMPV infection. (A) HAE tissues were treated with 2 μM SB105-A10 or vehicle (untreated) and infected with rgHMPV or rgPIV5 at an MOI of 5. Tissues were imaged at 48 h postinfection at ×5 magnification. (B) Quantification of HAE tissue infection. Data points are means ± the standard deviations of triplicate measurements and are representative of a minimum of three independent experiments.*, Statistical significance ($P < 0.0001$).

more, SB105-A10 has previously been reported to exhibit antiviral activity against RSV (54), CMV (61), HIV (62), HPV (63), and HSV-1 and HSV-2 (64), as well as some filoviruses (65).

To determine whether SB105-A10 reduces HMPV infection in human lung epithelial cells, BEAS-2B cells were treated with SB105-A10 at 1 μM prior to infection with rgHMPV at an MOI of 1, and the cells were imaged 24 h later for GFP expression; rgPIV5 was used in control studies to determine specificity. SB105-A10 treatment resulted in dramatic inhibition of HMPV infection, whereas PIV5 infection was not reduced (Fig. 6A). We performed quantification of the effects of SB105-A10 on rgHMPV or rgPIV5 infection by flow cytometry for GFP expression 24 h postinfection. In these experiments, both BEAS-2B and A549 cells were used to determine whether the effect of SB105-A10 is cell type-dependent, since this compound is mediating its effects by interacting with the target cell. In BEAS-2B cells, a dose-dependent inhibition of approximately 70% of rgHMPV infection resulted with SB105-A10 treatment, whereas rgPIV5 infection was not affected (Fig. 6B). Similar results were seen in A549 cells (Fig. 6C). In addition, treatment of BEAS-2B cells 2 μM SB105-A10, the highest concentration used in any cell or tissue experiments, did not reduce cell viability, as measured by an MTT cell viability assay (Fig. 6F). Based on our hypothesis of HMPV attachment, we predicted that SB105-A10 inhibits infection by blocking particle binding, specifically by preventing the interaction between heparan sulfate and F. To address this, we utilized a binding assay with WT HMPV, ΔG HMPV, and ΔGΔSH HMPV to determine the effects of SB105-A10. BEAS-2B cells were treated with 1 μM SB105-A10 or Opti-MEM prior to the addition of HMPV at an MOI of 1. The cells were incubated at 4°C for 2 h to allow for binding, and then cell lysates were analyzed for M by Western blotting to determine binding. A significant reduction in viral binding was observed in WT HMPV and the recombinant ΔG HMPV and ΔGΔSH HMPV with SB105-A10 treatment (Fig. 6D and E). As was observed in binding assays with iota-carrageenan (Fig. 2D), greater baseline binding was observed for ΔG HMPV and ΔGΔSH HMPV compared to the WT (Fig. 6D), although the same levels of reduction in binding were observed with SB105-A10 (Fig. 6E).

To determine the effect of SB105-A10 in polarized tissues, the apical surfaces of HAE tissues were treated with SB105-A10 at 2 μM prior to infection with rgHMPV or rgPIV5 at an MOI of 5. Treatment with SB105-A10 resulted in a reduction of HMPV infected cells 48 h postinfection, whereas PIV5 infection was not inhibited (Fig. 7A). Quantification of infected cells revealed a >50% reduction in HMPV infection at the apical surface with SB105-A10 treatment compared to vehicle-treated control tissues (Fig. 7B). Altogether, these results indicate that the occlusion of HS moieties on target cells inhibits HMPV binding and infection mediated by HMPV F and further support that HS is available for viral binding at the apical surface of the airway. Furthermore, based on our results, occlusion of HS could potentially be used as an antiviral strategy against HMPV.

DISCUSSION

Heparan sulfate is a key attachment factor for HMPV binding to the cell surface. In this study, we used compounds that modulate the attachment event to characterize the interaction between HMPV and HS. Our results support a model in which HMPV F mediates a direct binding interaction to HS, which can be inhibited by sulfated polysaccharides, specifically sulfated in the O position, and HS occluding compounds (Fig. 8). Whether these approaches can be used simultaneously to achieve greater inhibition of HMPV infection synergistically remains to be determined. Our results further indicate that HS in the airway epithelium serves as a binding factor during infection at the apical surface and suggest that HS modulating compounds may serve as a platform for potential HMPV antiviral development.

Iota-carrageenan treatment of HMPV resulted in inhibition of attachment (Fig. 2D) and infection (Fig. 2A and C) in bronchial epithelial cells and polarized airway tissues (Fig. 2F). The anti-HMPV activity of a sulfated polysaccharide has been previously reported using native and depolymerized galactans isolated from the red seaweed *Cryptonemia seminervis* (66). Although iota-carrageenan is a highly heterogeneous polysaccharide with regard to size, it is unclear whether its molecular mass is important in the inhibition of the viral interaction with heparan sulfate. It has been shown that depolymerized galactans ranging in molecular masses from 52 to 64 kDa were able to inhibit HMPV infection, as well as the intact polysaccharide, suggesting that low-molecular-mass sulfated polysaccharides can have potent antiviral activity (66). The potent anti-HMPV effect of iota-carrageenan on HMPV in-

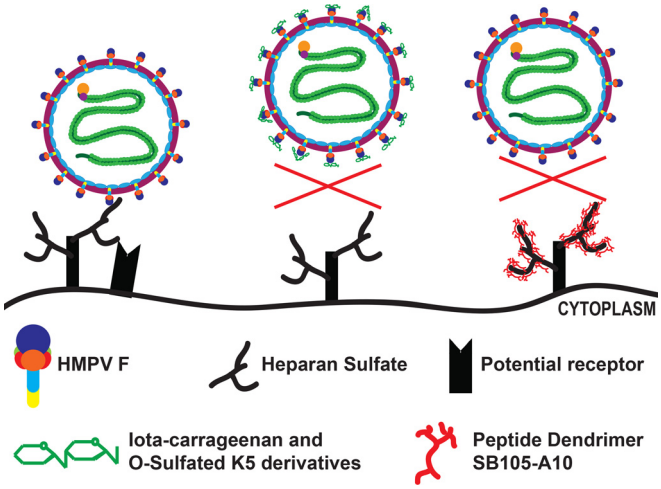

FIG 8 Model for inhibition of HMPV infection by interference between F and heparan sulfate. HMPV utilizes F for initial attachment to heparan sulfate found on the surface of target cells, with the potential involvement of an unidentified receptor necessary to complete entry. Sulfated polysaccharides, iota-carrageenan and the heparan sulfate-like K5 polysaccharide derivatives, inhibit this attachment step. Occluding heparan sulfate with SB105-A10 also blocks HMPV binding by occluding HS from interaction with HMPV F.

fection in both cells and tissue models has potential as a respiratory therapy, especially since iota-carrageenan has been shown to be safe to use in humans (46, 49, 67). Iota-carrageenan application in the form of a nasal spray in a randomized clinical trial, which included detection of rhinovirus, coronavirus types OC43 and 229E, influenza virus types A and B, HMPV, RSV, and PIV types 1, 2, and 3, led to a reduction in viral titers and fewer days of symptomatic illness (49). Its efficacy to specifically reduce HMPV infection in humans remains to be determined.

To better understand the structural features of heparan sulfate required for recognition by HMPV, we used a minilibrary of variably sulfated heparan-like K5 polysaccharide derivatives. Interestingly, our results highlight that variations in the structure of the K5 derivatives, namely, the position and degree of sulfation, can modulate the selectivity and potency of their activities against HMPV (Fig. 4B). The highly sulfated K5 polysaccharides exhibited the greatest inhibition of HMPV infection, suggesting that negative charges play a role in interacting with F (Fig. 4B). The highly sulfated K5-OS(H) and K5-N,OS(H) have been shown to inhibit dengue virus attachment to microvascular endothelial cells by interacting with the viral envelope protein, as shown by surface plasmon resonance (SPR) analysis using the receptor-binding domain III of the E protein (56). Our results support the model that HMPV binding to HS mediated by F involves charge-charge interaction, possibly by a cluster of exposed positively charged residues on F. This is demonstrated by the very high inhibitory activity exerted by K5-OS (H) (Fig. 4B, D, and E). This finding suggests the interaction between HMPV F and HS depends on a specific sulfation pattern rather than overall negative charges alone. Since the N-sulfated K5 derivatives are less effective in inhibiting the binding of HMPV, we can conclude that O-sulfate groups are important for HMPV F-HS interactions. Interestingly, the most effective fractions of depolymerized galactans to inhibit HMPV infection have the sulfate modifications principally on C-2 and C-6 of the galactose sugars (66). These results further support the importance of O-sulfate groups inhibiting the HS interaction with HMPV F and also suggest that the sugar backbone of the polysaccharide is not the main determinant of the antiviral activity. Furthermore, it has been shown RSV has entirely different sulfation requirements for binding to HS, since N-sulfation is required, whereas O-sulfation is dispensable (68), demonstrating that the binding between viruses and surface HSs are very specific.

Interestingly, binding experiments in the present study demonstrated a greater affinity of ΔG and ΔGΔSH HMPV to bind BEAS-2B cells than WT HMPV (Fig. 2D and 6D), since the untreated control bands consistently showed higher levels of particle binding for the recombinant viruses compared to the WT, despite equivalent number of particles added to the cells. Analysis for F content in the recombinant HMPV viruses did not reveal a greater F content relative to the M viral protein (Fig. 3D). We have previously reported that the ΔG and ΔGΔSH recombinant viruses bind and infect at WT levels in other cell types, suggesting that there may be cell-type-specific differences in binding. Taken together, these results suggest that SH and G negatively modulate binding in BEAS-2B cells, and thus their absence results in more efficient particle binding. Both HMPV SH and G have been previously reported to modulate events in HMPV entry. Our group has shown SH can modulate fusion activity of F (69). Furthermore, HMPV G and SH have been previously shown to negatively modulate HMPV entry, as particle uptake by micropinocytosis in dendritic cells is enhanced for recombinant HMPV lacking G and SH (70). Soluble HMPV G has been shown to bind HS *in vitro* (71), which suggests that it may have some interaction with HS at the surfaces of cells and the apical surfaces of HAE cultures. However, results in monolayer cells suggest that HMPV F is the principal driver of particle interaction with HS (Fig. 2D). Further studies with recombinant HMPV lacking G and/or SH are necessary to determine what role these proteins may play during the critical early steps in HMPV infection of cell culture and HAE model systems.

Treating the cells and tissues with SB105-A10, which specifically occludes any ligand binding to HSPGs, resulted in a significant inhibition of HMPV binding and infection. Our results further support the model that HMPV uses HS as an attachment factor due to a direct binding interaction with F. While adhered immortalized cells readily express accessible heparan sulfate, it is less clear where HS localizes in the respiratory epithelium *in vivo*. Based on detection by immunohistochemistry of human epithelial tissue, heparan sulfate has been previously hypothesized to localize exclusively to the basolateral epithelium (50), making it unclear how a respiratory virus would access HS to infect apically. The results in this study demonstrate that HMPV can infect polarized airway tissues at the apical surface and that HS occlusion inhibits this apical infection, suggesting that HS is found at sufficient levels to promote attachment at the apical surface of the airway. HS occlusion with SB105-A10 has also been shown to inhibit RSV infection at the apical surfaces of HAE tissues (54). HS modification is found on a number of transmembrane proteins, and the two main protein families with HS are syndecans and glypicans. Syndecans have been shown to serve as receptors for other HS-binding viruses, including hepatitis C virus (72), dengue virus (73), and HIV (30). Anti-syndecan-1 antibodies have recently been shown to block RSV infection at the apical surface of human airway epithelium cultures (74). The role of a specific HSPG, such as one of the syndecan proteins, in HMPV infection

remains to be determined, but our results strongly indicate that sufficient levels of HS on HSPGs are exposed at the apical surface of the airway epithelium for viral infection, including infection with HMPV.

ACKNOWLEDGMENTS

We thank members of the Dutch lab for discussions and evaluations of experiments and the manuscript.

Research reported in this publication was supported by the National Institute of Allergy and Infectious Diseases of the National Institutes of Health (NIH) under award F30AI114194 to E.M.K. and NIH grants R01AI051517 and 2P20 RR020171 from the National Center for Research Resources to R.E.D. Funding was also provided by the CCTS TL1 training program (TL1TR000115) to E.M.K. and UK University Research Professor funds to R.E.D. The UK Flow Cytometry & Cell Sorting Core facility is supported in part by the Office of the Vice President for Research, the Markey Cancer Center, and an NCI Center Core Support Grant (P30 CA177558) to the University of Kentucky Markey Cancer Center.

E.M.K., S.E.S., P.O., D.L., and R.E.D. conceived and designed the experiments. E.M.K. and S.E.S. performed the experiments. E.M.K., S.E.S., P.O., D.L., and R.E.D. analyzed the data. P.O., D.L., and R.E.D. contributed reagents, materials, and/or analysis tools. E.M.K., D.L., P.O., and R.E.D. wrote the paper.

The content is solely the responsibility of the authors and does not necessarily represent the official views of the National Institutes of Health.

FUNDING INFORMATION

This work, including the efforts of Edita Klimyte, was funded by HHS | National Institutes of Health (NIH) (F30AI114194 and TL1TR000115). This work, including the efforts of Rebecca Ellis Dutch, was funded by HHS | National Institutes of Health (NIH) (R01AI051517 and 2P20 RR020171).

REFERENCES

1. **Monto AS.** 2002. Epidemiology of viral respiratory infections. Am J Med **112**(Suppl 6A)**:**4S–12S.
2. **van den Hoogen BG, de Jong JC, Groen J, Kuiken T, de Groot R, Fouchier RA, Osterhaus AD.** 2001. A newly discovered human pneumovirus isolated from young children with respiratory tract disease. Nat Med **7:**719–724. http://dx.doi.org/10.1038/89098.
3. **van den Hoogen BG, van Doornum GJ, Fockens JC, Cornelissen JJ, Beyer WE, de Groot R, Osterhaus AD, Fouchier RA.** 2003. Prevalence and clinical symptoms of human metapneumovirus infection in hospitalized patients. J Infect Dis **188:**1571–1577. http://dx.doi.org/10.1086/379200.
4. **van den Hoogen BG, Osterhaus DM, Fouchier RA.** 2004. Clinical impact and diagnosis of human metapneumovirus infection. Pediatr Infect Dis J **23:**S25–S32. http://dx.doi.org/10.1097/01.inf.0000108190.09824.e8.
5. **Don M, Korppi M, Valent F, Vainionpaa R, Canciani M.** 2008. Human metapneumovirus pneumonia in children: results of an Italian study and mini-review. Scand J Infect Dis **40:**821–826. http://dx.doi.org/10.1080/00365540802227110.
6. **Kahn JS.** 2006. Epidemiology of human metapneumovirus. Clin Microbiol Rev **19:**546–557. http://dx.doi.org/10.1128/CMR.00014-06.
7. **Deffrasnes C, Hamelin ME, Boivin G.** 2007. Human metapneumovirus. Semin Respir Crit Care Med **28:**213–221. http://dx.doi.org/10.1055/s-2007-976493.
8. **Boivin G, De Serres G, Cote S, Gilca R, Abed Y, Rochette L, Bergeron MG, Dery P.** 2003. Human metapneumovirus infections in hospitalized children. Emerg Infect Dis **9:**634–640. http://dx.doi.org/10.3201/eid0906.030017.
9. **Esper F, Boucher D, Weibel C, Martinello RA, Kahn JS.** 2003. Human metapneumovirus infection in the United States: clinical manifestations associated with a newly emerging respiratory infection in children. Pediatrics **111:**1407–1410. http://dx.doi.org/10.1542/peds.111.6.1407.
10. **Esper F, Martinello RA, Boucher D, Weibel C, Ferguson D, Landry ML, Kahn JS.** 2004. A 1-year experience with human metapneumovirus in children aged <5 years. J Infect Dis **189:**1388–1396. http://dx.doi.org/10.1086/382482.
11. **Feuillet F, Lina B, Rosa-Calatrava M, Boivin G.** 2012. Ten years of human metapneumovirus research. J Clin Virol **53:**97–105. http://dx.doi.org/10.1016/j.jcv.2011.10.002.
12. **Schildgen O, Glatzel T, Geikowski T, Scheibner B, Matz B, Bindl L, Born M, Viazov S, Wilkesmann A, Knopfle G, Roggendorf M, Simon A.** 2005. Human metapneumovirus RNA in encephalitis patient. Emerg Infect Dis **11:**467–470. http://dx.doi.org/10.3201/eid1103.040676.
13. **Arnold JC, Singh KK, Milder E, Spector SA, Sawyer MH, Gavali S, Glaser C.** 2009. Human metapneumovirus associated with central nervous system infection in children. Pediatr Infect Dis J **28:**1057–1060. http://dx.doi.org/10.1097/INF.0b013e3181acd221.
14. **Niizuma T, Okumura A, Kinoshita K, Shimizu T.** 2014. Acute encephalopathy associated with human metapneumovirus infection. Jpn J Infect Dis **67:**213–215. http://dx.doi.org/10.7883/yoken.67.213.
15. **Weinreich, MA, Jabbar AY, Malguria N, Haley RW.** 2015. New-onset myocarditis in an immunocompetent adult with acute metapneumovirus infection. Case Rep Med **2015:**814269.
16. **Principi N, Esposito S.** 2014. Paediatric human metapneumovirus infection: epidemiology, prevention, and therapy. J Clin Virol **59:**141–147. http://dx.doi.org/10.1016/j.jcv.2014.01.003.
17. **Chang A, Masante C, Buchholz UJ, Dutch RE.** 2012. Human metapneumovirus (HMPV) binding and infection are mediated by interactions between the HMPV fusion protein and heparan sulfate. J Virol **86:**3230–3243. http://dx.doi.org/10.1128/JVI.06706-11.
18. **Cox RG, Mainou BA, Johnson M, Hastings AK, Schuster JE, Dermody TS, Williams JV.** 2015. Human metapneumovirus is capable of entering cells by fusion with endosomal membranes. PLoS Pathog **11:**e1005303. http://dx.doi.org/10.1371/journal.ppat.1005303.
19. **Cseke G, Maginnis MS, Cox RG, Tollefson SJ, Podsiad AB, Wright DW, Dermody TS, Williams JV.** 2009. Integrin αvβ1 promotes infection by human metapneumovirus. Proc Natl Acad Sci U S A **106:**1566–1571. http://dx.doi.org/10.1073/pnas.0801433106.
20. **Cox RG, Livesay SB, Johnson M, Ohi MD, Williams JV.** 2012. The human metapneumovirus fusion protein mediates entry via an interaction with RGD-binding integrins. J Virol **86:**12148–12160. http://dx.doi.org/10.1128/JVI.01133-12.
21. **Feldman SA, Audet S, Beeler JA.** 2000. The fusion glycoprotein of human respiratory syncytial virus facilitates virus attachment and infectivity via an interaction with cellular heparan sulfate. J Virol **74:**6442–6447. http://dx.doi.org/10.1128/JVI.74.14.6442-6447.2000.
22. **Hallak LK, Collins PL, Knudson W, Peeples ME.** 2000. Iduronic acid-containing glycosaminoglycans on target cells are required for efficient respiratory syncytial virus infection. Virology **271:**264–275. http://dx.doi.org/10.1006/viro.2000.0293.
23. **Escribano-Romero E, Rawling J, Garcia-Barreno B, Melero JA.** 2004. The soluble form of human respiratory syncytial virus attachment protein differs from the membrane-bound form in its oligomeric state but is still capable of binding to cell surface proteoglycans. J Virol **78:**3524–3532. http://dx.doi.org/10.1128/JVI.78.7.3524-3532.2004.
24. **Giroglou T, Florin L, Schafer F, Streeck RE, Sapp M.** 2001. Human papillomavirus infection requires cell surface heparan sulfate. J Virol **75:**1565–1570. http://dx.doi.org/10.1128/JVI.75.3.1565-1570.2001.
25. **WuDunn D, Spear PG.** 1989. Initial interaction of herpes simplex virus with cells is binding to heparan sulfate. J Virol **63:**52–58.
26. **Shieh MT, WuDunn D, Montgomery RI, Esko JD, Spear PG.** 1992. Cell surface receptors for herpes simplex virus are heparan sulfate proteoglycans. J Cell Biol **116:**1273–1281. http://dx.doi.org/10.1083/jcb.116.5.1273.
27. **Herold BC, Visalli RJ, Susmarski N, Brandt CR, Spear PG.** 1994. Glycoprotein C-independent binding of herpes simplex virus to cells requires cell surface heparan sulfate and glycoprotein B J Gen Virol **75:**1211–1222.
28. **Shukla D, Liu J, Blaiklock P, Shworak NW, Bai X, Esko JD, Cohen GH, Eisenberg RJ, Rosenberg RD, Spear PG.** 1999. A novel role for 3-O-sulfated heparan sulfate in herpes simplex virus 1 entry. Cell **99:**13–22. http://dx.doi.org/10.1016/S0092-8674(00)80058-6.
29. **Patel M, Yanagishita M, Roderiquez G, Bou-Habib DC, Oravecz T, Hascall VC, Norcross MA.** 1993. Cell-surface heparan sulfate proteoglycan mediates HIV-1 infection of T-cell lines. AIDS Res Hum Retroviruses **9:**167–174. http://dx.doi.org/10.1089/aid.1993.9.167.
30. **de Witte L, Bobardt M, Chatterji U, Degeest G, David G, Geijtenbeek TB, Gallay P.** 2007. Syndecan-3 is a dendritic cell-specific attachment

receptor for HIV-1. Proc Natl Acad Sci U S A **104:**19464–19469. http://dx.doi.org/10.1073/pnas.0703747104.
31. **Crublet E, Andrieu JP, Vives RR, Lortat-Jacob H.** 2008. The HIV-1 envelope glycoprotein gp120 features four heparan sulfate binding domains, including the coreceptor binding site. J Biol Chem **283:**15193–15200. http://dx.doi.org/10.1074/jbc.M800066200.
32. **Spillmann D.** 2001. Heparan sulfate: anchor for viral intruders? Biochimie **83:**811–817. http://dx.doi.org/10.1016/S0300-9084(01)01290-1.
33. **Biacchesi S, Skiadopoulos MH, Yang L, Lamirande EW, Tran KC, Murphy BR, Collins PL, Buchholz UJ.** 2004. Recombinant human Metapneumovirus lacking the small hydrophobic SH and/or attachment G glycoprotein: deletion of G yields a promising vaccine candidate. J Virol **78:**12877–12887. http://dx.doi.org/10.1128/JVI.78.23.12877-12887.2004.
34. **Biacchesi S, Pham QN, Skiadopoulos MH, Murphy BR, Collins PL, Buchholz UJ.** 2005. Infection of nonhuman primates with recombinant human metapneumovirus lacking the SH, G, or M2-2 protein categorizes each as a nonessential accessory protein and identifies vaccine candidates. J Virol **79:**12608–12613. http://dx.doi.org/10.1128/JVI.79.19.12608-12613.2005.
35. **Schowalter RM, Chang A, Robach JG, Buchholz UJ, Dutch RE.** 2009. Low-pH triggering of human metapneumovirus fusion: essential residues and importance in entry. J Virol **83:**1511–1522. http://dx.doi.org/10.1128/JVI.01381-08.
36. **Sabo Y, Ehrlich M, Bacharach E.** 2011. The conserved YAGL motif in human metapneumovirus is required for higher-order cellular assemblies of the matrix protein and for virion production. J Virol **85:**6594–6609. http://dx.doi.org/10.1128/JVI.02694-10.
37. **Schowalter RM, Smith SE, Dutch RE.** 2006. Characterization of human metapneumovirus F protein-promoted membrane fusion: critical roles for proteolytic processing and low pH. J Virol **80:**10931–10941. http://dx.doi.org/10.1128/JVI.01287-06.
38. **Leali D, Belleri M, Urbinati C, Coltrini D, Oreste P, Zoppetti G, Ribatti D, Rusnati M, Presta M.** 2001. Fibroblast growth factor-2 antagonist activity and angiostatic capacity of sulfated *Escherichia coli* K5 polysaccharide derivatives. J Biol Chem **276:**37900–37908.
39. **Biacchesi S, Murphy BR, Collins PL, Buchholz UJ.** 2007. Frequent frameshift and point mutations in the SH gene of human metapneumovirus passaged in vitro. J Virol **81:**6057–6067. http://dx.doi.org/10.1128/JVI.00128-07.
40. **Paterson RG, Lamb RA.** 1993. The molecular biology of influenza viruses and paramyxoviruses, p 35–73. *In* Davidson A, Elliott RM (ed), Molecular virology: a practical approach. IRL Oxford University Press, Oxford, United Kingdom.
41. **de Graaf M, Herfst S, Aarbiou J, Burgers PC, Zaaraoui-Boutahar F, Bijl M, van Ijcken W, Schrauwen EJ, Osterhaus AD, Luider TM, Scholte BJ, Fouchier RA, Andeweg AC.** 2013. Small hydrophobic protein of human metapneumovirus does not affect virus replication and host gene expression in vitro. PLoS One **8:**e58572. http://dx.doi.org/10.1371/journal.pone.0058572.
42. **Ahmadi A, Zorofchian-Moghadamtousi S, Abubakar S, Zandi K.** 2015. Antiviral potential of algae polysaccharides isolated from marine sources: a review. Biomed Res Int **2015:**825203.
43. **Buck CB, Thompson CD, Roberts JN, Muller M, Lowy DR, Schiller JT.** 2006. Carrageenan is a potent inhibitor of papillomavirus infection. PLoS Pathog **2:**e69. http://dx.doi.org/10.1371/journal.ppat.0020069.
44. **Lynch G, Low L, Li S, Sloane A, Adams S, Parish C, Kemp B, Cunningham AL.** 1994. Sulfated polyanions prevent HIV infection of lymphocytes by disruption of the CD4-gp120 interaction, but do not inhibit monocyte infection. J Leukoc Biol **56:**266–272.
45. **Talarico LB, Noseda MD, Ducatti DR, Duarte ME, Damonte EB.** 2011. Differential inhibition of dengue virus infection in mammalian and mosquito cells by iota-carrageenan. J Gen Virol **92:**1332–1342. http://dx.doi.org/10.1099/vir.0.028522-0.
46. **Leibbrandt A, Meier C, Konig-Schuster M, Weinmullner R, Kalthoff D, Pflugfelder B, Graf P, Frank-Gehrke B, Beer M, Fazekas T, Unger H, Prieschl-Grassauer E, Grassauer A.** 2010. Iota-carrageenan is a potent inhibitor of influenza A virus infection. PLoS One **5:**e14320. http://dx.doi.org/10.1371/journal.pone.0014320.
47. **Eccles R, Meier C, Jawad M, Weinmullner R, Grassauer A, Prieschl-Grassauer E.** 2010. Efficacy and safety of an antiviral Iota-Carrageenan nasal spray: a randomized, double-blind, placebo-controlled exploratory study in volunteers with early symptoms of the common cold. Respir Res **11:**108. http://dx.doi.org/10.1186/1465-9921-11-108.
48. **Fazekas T, Eickhoff P, Pruckner N, Vollnhofer G, Fischmeister G, Diakos C, Rauch M, Verdianz M, Zoubek A, Gadner H, Lion T.** 2012. Lessons learned from a double-blind randomised placebo-controlled study with a iota-carrageenan nasal spray as medical device in children with acute symptoms of common cold. BMC Comp Altern Med **12:**147. http://dx.doi.org/10.1186/1472-6882-12-147.
49. **Ludwig M, Enzenhofer E, Schneider S, Rauch M, Bodenteich A, Neumann K, Prieschl-Grassauer E, Grassauer A, Lion T, Mueller CA.** 2013. Efficacy of a carrageenan nasal spray in patients with common cold: a randomized controlled trial. Respir Res **14:**124. http://dx.doi.org/10.1186/1465-9921-14-124.
50. **Hayashi K, Hayashi M, Jalkanen M, Firestone JH, Trelstad RL, Bernfield M.** 1987. Immunocytochemistry of cell surface heparan sulfate proteoglycan in mouse tissues: a light and electron microscopic study. J Histochem Cytochem **35:**1079–1088. http://dx.doi.org/10.1177/35.10.2957423.
51. **Palmer SG, Porotto M, Palermo LM, Cunha LF, Greengard O, Moscona A.** 2012. Adaptation of human parainfluenza virus to airway epithelium reveals fusion properties required for growth in host tissue. mBio **3:**e00137-12. http://dx.doi.org/10.1128/mBio.00137-12.
52. **Bai J, Smock SL, Jackson GR, Jr, MacIsaac KD, Huang Y, Mankus C, Oldach J, Roberts B, Ma YL, Klappenbach JA, Crackower MA, Alves SE, Hayden PJ.** 2015. Phenotypic responses of differentiated asthmatic human airway epithelial cultures to rhinovirus. PLoS One **10:**e0118286. http://dx.doi.org/10.1371/journal.pone.0118286.
53. **Deng X, Li Y, Qiu J.** 2014. Human bocavirus 1 infects commercially available primary human airway epithelium cultures productively. J Virol Methods **195:**112–119. http://dx.doi.org/10.1016/j.jviromet.2013.10.012.
54. **Donalisio M, Rusnati M, Cagno V, Civra A, Bugatti A, Giuliani A, Pirri G, Volante M, Papotti M, Landolfo S, Lembo D.** 2012. Inhibition of human respiratory syncytial virus infectivity by a dendrimeric heparan sulfate-binding peptide. Antimicrob Agents Chemother **56:**5278–5288. http://dx.doi.org/10.1128/AAC.00771-12.
55. **Cagno V, Donalisio M, Civra A, Volante M, Veccelli E, Oreste P, Rusnati M, Lembo D.** 2014. Highly sulfated K5 *Escherichia coli* polysaccharide derivatives inhibit respiratory syncytial virus infectivity in cell lines and human tracheal-bronchial histocultures. Antimicrob Agents Chemother **58:**4782–4794. http://dx.doi.org/10.1128/AAC.02594-14.
56. **Vervaeke P, Alen M, Noppen S, Schols D, Oreste P, Liekens S.** 2013. Sulfated *Escherichia coli* K5 polysaccharide derivatives inhibit dengue virus infection of human microvascular endothelial cells by interacting with the viral envelope protein E domain III. PLoS One **8:**e74035. http://dx.doi.org/10.1371/journal.pone.0074035.
57. **Mercorelli B, Oreste P, Sinigalia E, Muratore G, Lembo D, Palu G, Loregian A.** 2010. Sulfated derivatives of *Escherichia coli* K5 capsular polysaccharide are potent inhibitors of human cytomegalovirus. Antimicrob Agents Chemother **54:**4561–4567. http://dx.doi.org/10.1128/AAC.00721-10.
58. **Pinna D, Oreste P, Coradin T, Kajaste-Rudnitski A, Ghezzi S, Zoppetti G, Rotola A, Argnani R, Poli G, Manservigi R, Vicenzi E.** 2008. Inhibition of herpes simplex virus types 1 and 2 in vitro infection by sulfated derivatives of *Escherichia coli* K5 polysaccharide. Antimicrob Agents Chemother **52:**3078–3084. http://dx.doi.org/10.1128/AAC.00359-08.
59. **Vicenzi E, Gatti A, Ghezzi S, Oreste P, Zoppetti G, Poli G.** 2003. Broad spectrum inhibition of HIV-1 infection by sulfated K5 *Escherichia coli* polysaccharide derivatives. AIDS **17:**177–181. http://dx.doi.org/10.1097/00002030-200301240-00006.
60. **Esko JD, Selleck SB.** 2002. Order out of chaos: assembly of ligand binding sites in heparan sulfate. Annu Rev Biochem **71:**435–471. http://dx.doi.org/10.1146/annurev.biochem.71.110601.135458.
61. **Luganini A, Giuliani A, Pirri G, Pizzuto L, Landolfo S, Gribaudo G.** 2010. Peptide-derivatized dendrimers inhibit human cytomegalovirus infection by blocking virus binding to cell surface heparan sulfate. Antiviral Res **85:**532–540. http://dx.doi.org/10.1016/j.antiviral.2010.01.003.
62. **Bon I, Lembo D, Rusnati M, Clo A, Morini S, Miserocchi A, Bugatti A, Grigolon S, Musumeci G, Landolfo S, Re MC, Gibellini D.** 2013. Peptide-derivatized SB105-A10 dendrimer inhibits the infectivity of R5 and X4 HIV-1 strains in primary PBMCs and cervicovaginal histocultures. PLoS One **8:**e76482. http://dx.doi.org/10.1371/journal.pone.0076482.
63. **Donalisio M, Rusnati M, Civra A, Bugatti A, Allemand D, Pirri G, Giuliani A, Landolfo S, Lembo D.** 2010. Identification of a dendrimeric heparan sulfate-binding peptide that inhibits infectivity of genital types of

human papillomaviruses. Antimicrob Agents Chemother **54:**4290–4299. http://dx.doi.org/10.1128/AAC.00471-10.
64. **Luganini A, Nicoletto SF, Pizzuto L, Pirri G, Giuliani A, Landolfo S, Gribaudo G.** 2011. Inhibition of herpes simplex virus type 1 and type 2 infections by peptide-derivatized dendrimers. Antimicrob Agents Chemother **55:**3231–3239. http://dx.doi.org/10.1128/AAC.00149-11.
65. **Salvador B, Sexton NR, Carrion R, Jr, Nunneley J, Patterson JL, Steffen I, Lu K, Muench MO, Lembo D, Simmons G.** 2013. Filoviruses utilize glycosaminoglycans for their attachment to target cells. J Virol **87:**3295–3304. http://dx.doi.org/10.1128/JVI.01621-12.
66. **Mendes GS, Duarte ME, Colodi FG, Noseda MD, Ferreira LG, Berte SD, Cavalcanti JF, Santos N, Romanos MT.** 2014. Structure and anti-metapneumovirus activity of sulfated galactans from the red seaweed *Cryptonemia seminervis*. Carbohydr Polymers **101:**313–323. http://dx.doi.org/10.1016/j.carbpol.2013.09.026.
67. **Grassauer A, Weinmuellner R, Meier C, Pretsch A, Prieschl-Grassauer E, Unger H.** 2008. Iota-carrageenan is a potent inhibitor of rhinovirus infection. Virol J **5:**107. http://dx.doi.org/10.1186/1743-422X-5-107.
68. **Hallak LK, Spillmann D, Collins PL, Peeples ME.** 2000. Glycosaminoglycan sulfation requirements for respiratory syncytial virus infection. J Virol **74:**10508–10513. http://dx.doi.org/10.1128/JVI.74.22.10508-10513.2000.
69. **Masante C, El Najjar F, Chang A, Jones A, Moncman CL, Dutch RE.** 2014. The human metapneumovirus small hydrophobic protein has properties consistent with those of a viroporin and can modulate viral fusogenic activity. J Virol **88:**6423–6433. http://dx.doi.org/10.1128/JVI.02848-13.
70. **Le Nouen C, Hillyer P, Brock LG, Winter CC, Rabin RL, Collins PL, Buchholz UJ.** 2014. Human metapneumovirus SH and G glycoproteins inhibit macropinocytosis-mediated entry into human dendritic cells and reduce $CD4^+$ T cell activation. J Virol **88:**6453–6469. http://dx.doi.org/10.1128/JVI.03261-13.
71. **Thammawat S, Sadlon TA, Hallsworth PG, Gordon DL.** 2008. Role of cellular glycosaminoglycans and charged regions of viral G protein in human metapneumovirus infection. J Virol **82:**11767–11774. http://dx.doi.org/10.1128/JVI.01208-08.
72. **Shi Q, Jiang J, Luo G.** 2013. Syndecan-1 serves as the major receptor for attachment of hepatitis C virus to the surfaces of hepatocytes. J Virol **87:**6866–6875. http://dx.doi.org/10.1128/JVI.03475-12.
73. **Okamoto K, Kinoshita H, Parquet Mdel C, Raekiansyah M, Kimura D, Yui K, Islam MA, Hasebe F, Morita K.** 2012. Dengue virus strain DEN2 16681 utilizes a specific glycochain of syndecan-2 proteoglycan as a receptor. J Gen Virol **93:**761–770. http://dx.doi.org/10.1099/vir.0.037853-0.
74. **Chirkova T, Lin S, Oomens AG, Gaston KA, Boyoglu-Barnum S, Meng J, Stobart CC, Cotton CU, Hartert TV, Moore ML, Ziady AG, Anderson LJ.** 2015. CX3CR1 is an important surface molecule for respiratory syncytial virus infection in human airway epithelial cells. J Gen Virol **96:**2543–2556. http://dx.doi.org/10.1099/vir.0.000218.